Studying Chaotic Modeling for Earthquake Prediction (An Overview: NW of Iran)

R. Mehrnia

Assistant Professor, Payame Noor University (PNU), Tehran, I.R. Iran,
email: r_mehrniya@pnu.ac.ir

ABSTRACT

Recently, many geoscientists have focused on chaos and its relevant subjects for understanding nonlinearity of nature as the main criteria in explaining the dynamic behavior of earthquakes, mineralization and other similar processes. Mathematically, the multivariate iterative functions have basic fractal expression in the analytical, practical and computational domains. In this research, a dynamic model of geophysical precursors is presented, using logistic map, to describe simply the complexities at the edge of chaos. In the proposed model, the seismic, magnetic, gravimetric and electromagnetic data are included. Here, the research region is divided into stable and active areas, according to the historical earthquakes. In this regard, in the Eastern Azerbaijan province around Anatolian fault system, the μ parameter values are used as the average net reproductive rate values. The results show evidential themes containing independent variables in eighteen integrated model cells. Also fourteen forecast cells can be determined after applying the net values into the regions of lower priorities, with or without potential for future events, in comparison with model cells.

Keywords:
Chaotic model;
Earthquake prediction;
Fractals;
Geophysical data

1. Introduction

Chaos theory has provided unique explanation for different high complex phenomena that may have simple mechanisms at the beginning but at the middle or final stages they strike more problematic appearances. For example, to describe pre-seismic dataset precisely might be out of reach for estimating the time, location and magnitude of next events. In such conditions, chaos as, the irregular behavior of a natural system, provides a link between simple deterministic and random processes for modeling the complex variations according to the events.

As a rule, the mathematical iterations indicate that the formation of complexities is controlled by some processes. Therefore, understanding fractal geometry is necessary in the foundation of recursive functions to describe the bifurcative peculiarities at the edge of chaos [1].

A cubic model for illustrating fragmentation processes under deterministic chaos is shown in Figure (1). In this figure, the cubic spaces of media are divided into equal linear dimensions (h) as the cell values [2]. This cell is divided into eight isometric elements of (h/2) dimension. Each fragmented element (with h/2 dimension) is considered as the first order initial cell.

Following subdivision, new elements of h/4 dimensions are formed among the series of fragmentations. All these can be presented in the form of probability function assumption (f) for the first order cells under repeated statement of the first orderly elements (e.g. coefficient of number 8). It satisfies Eq. (1) as relative logarithmic expression to fractal distributions

$$D = 3\ ln\ (8f)\ /\ ln\ 8 \qquad (1)$$

where, D is the ideal factor for modeling fragmented

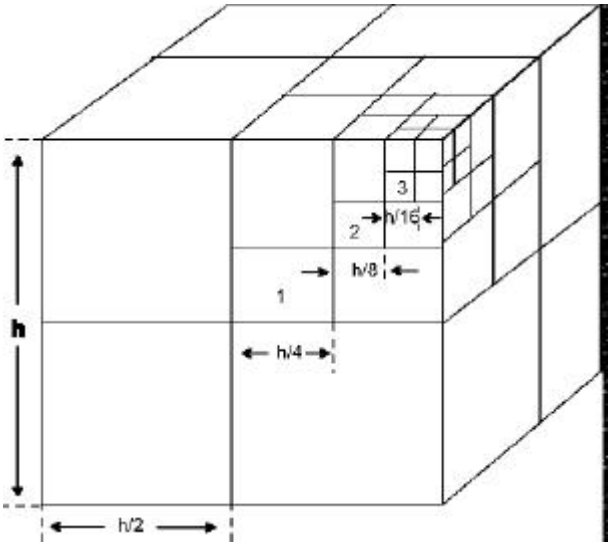

Figure 1. Theoretical model for deterministic chaos. Fragmentation properties into first order elements with the dimension of h/2, h/4, h/16, etc.

(fractal) distribution of variables under exponential logarithmic *"ln"* relationships with probabilistic functions [2].

If it is possible to model the variations using simple equations, the prognosis of the future fluctuations (e.g. main shocks related to seismic alternatives) is available as well. In this regard simple functions are used for separating multifractal populations based on nonlinear characteristics of chaos in discrete short time periods [1].

Due to nonlinearity effects, a few degrees of freedom is needed for generating chaotic motions [3]. The chaos behavior can be modeled, after the motions, according to the deterministic conceptual models.

In practice the predictive chaos with dynamic specifications is better than linear stochastic model which refers to the long run unpredictable effects.

Geologically, the earth is considered as dissipative conformation which gradually undergoes huge actions with nonlinear aspects [4].

The concept of chaos dynamics has been concerned in geology by Turcotte [5] to understand how strong uneven characteristics appear in the underground materials because of nonlinearity. In the real world, evolution is the natural response to the fighting and interaction between parameters and circumstances until meeting self adaptation in the systems for more surviving and extending their development in the changeable environments.

This paper consists of three sections:

1. The empirical relationships between chaos and seismicity;
2. The overview of chaotic conceptual models regarding seismic precursory evidences, a brief case study of Anatolian earthquakes;
3. The summarized conclusions and suggestions for future studies in *NW* of Iran.

2. Fractal Distribution of Earthquakes

Based on Gutenberg-Richter empirical equation, in most cases, the number of earthquakes (*N*) with the magnitudes greater than *m* satisfies the linear relationship as Eq. (2):

$$Log\ N = -b\ m + a \tag{2}$$

where, *a* and *b* are constant for surfacing magnitudes as restricted waves. This equation is applicable in local and regional (world wide) scales. The *b*-value is used as regional measuring of seismicity and is equivalent assumption for defining fractal dimensions in the edge of chaos [3].

The earthquakes' moments are defined by Eq. (3) as below:

$$M = \theta \delta A \tag{3}$$

where, θ is the shear modulus, δ is mean displacement of active fault system; and *A* is the rupture's surface. This equation can be related to magnitude values, shown in Eq. (4):

$$log\, M = 1.5m + d \tag{4}$$

where *d* is an empirical constant.

After Kanamori earthquake (1975), Turcotte [5] emphasized that the earthquakes' moments *"M"* have power law relationships with linear dimension because of definite crustal ruptures *"r = $A^{1/2}$"* as presented in Eq. (5):

$$M = \lambda r^3 = \lambda (A^{0.5})^3 = \lambda A^{3/2} \tag{5}$$

Combining the Eqs (2), (4) and (5), Eq. (6) is obtained as below:

$$Log\, N = -2b\, log\, r + \beta \tag{6}$$

where,

$$\beta = [(bd / 1.5) + a] - [b/1.5]\, log\, a$$

Eq. (6) can be rewritten in the form of Eq. (7) as follows:

$$N = \beta r^{-2b} \tag{7}$$

Eq. (6) is a nonlinear relationship with the power

= -2*b* equivalent to the fractal dimension (*D*), shown in Eq. (8):

$$D = 2b \quad (8)$$

According to the above formula, *D*-values are twice *b*-values, studying the regional seismic activities based on frequency-magnitude (*F-M*) fractal equations [5].

Regional seismicity in the *NW* of Iran is an example of empirical *F-M* distribution on the basis of data in 1978-2008. Here the number of Anatolian earthquakes per year (*N*) are shown versus interpolated (surfacing) magnitudes which are greater than *m*. This *m* value is the result of functional measurements around the north fault of Tabriz.

According to Figure (2), the magnitude ranges of $3.85 < m < 5.90$ are really compatible with Eq. (1) where, $b = 0.71$ or $D = 1.42$ with $d = 18$ and $\lambda = 3.30\text{x}107 dyne/cm^2$ for corresponding estimated values of $r = 1.5^{-10} km$..

Regarding the magnitude less than 3.85, broad instrumental coverage are needed for detail evaluation of regions which may meet inadequate supplements.

Anatolian catalogues are apparently deviated from *F-M* fractal correlations in the magnitudes greater than 5.90. This is because of rare historical seismic events or significant statistical evidences which may appear out of ordered similarities as the result of asymmetrical fault breaking processes in the larger earthquakes.

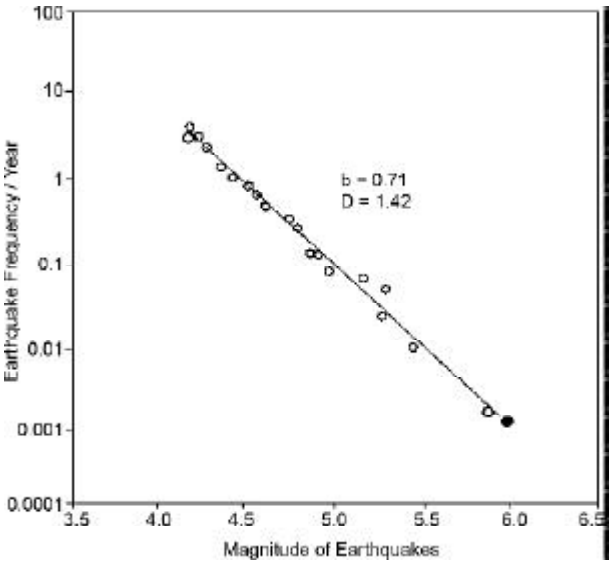

Figure 2. Frequency- magnitude distribution of Anatolian earthquakes. Open circles are IIEES data, catalogue from 1978 to 2008, solid circle is the expected rate of seismic activities greater than previous hazardous event.

There is meaningful relationship between the number of earthquakes (*N*) and larger events occurred in the north of Tabriz. Therefore, a new fractal extrapolation is proposed for regional seismicity of some hazardous areas in the eastern territories of Anatolian fault system. This fact is a reasonable prediction of greater earthquakes in the future. Earthquake prediction is completely sensitive to *b*-values as the slope of linear distributions in certain regions. In cases where the slopes remain constant, still there is no evidence of seismicity variations in time domain that the new level of earthquake potential may appear [5].

The largest earthquake in any region has important role in the fractal distribution of magnitudes. It means that the great earthquake reduces the stress level over a larger region and therefore the seismicity is reduced as the dependent variable of magnitudes. The largest earthquakes impose some extended side effects which are related to the structural patterns and can be observed in the regional scales. In other words, seismic hazard depends completely on the magnitude of largest earthquake in each region [5].

Tectonic models are needed for better understanding of fractal distributions related to seismic events. Therefore, in ideal cases, fractal dimension of active fault system can be recognized by fractal dimension of earthquakes in any region free of scales.

3. Mathematical Statements for Seismic Nonlinearity

In geological environments, the main pattern of structures may refer to active fault zones which are candidates for initiating small or big motions before and after earthquakes. Cross cutting locations are usually responsible for starting pre-seismic activities before the main shocks with magnitudes greater than 6 ($M > 6$), seen practically in the recent and some historical events.

Charging and discharging of stresses control the rupturing of magnitudes, times and locations in some regions. Here, they are supposed constant; then, charging potentials are calculated by Eq. (9) as mentioned below:

$$\{[X(t+\delta t) - X(t)]/\delta t\}_{charging} = cCX(t) \quad (9)$$

where,

$X(t)$= stress parameter in a district at time t;

c, greater than zero, is the charging rate of effective forces (stress);

C is constant parameter referring to the quantity of historical inherent potential;

δt is time increment.

Meanwhile, the mathematical relationship for discharging (shock events) is defined by Eq. (10).

$$\{[X(t+\delta t) - X(t)]/\delta t\}_{discharging} = -dX(t) \quad (10)$$

Where, d, greater than zero, is the discharging rate of effective forces in definite regions.

The Eqs. (9) and (10) are combined and Eq. (11) is obtained as below:

$$\{[X(t+\delta t) - X(t)]/\delta t\} = cCX(t) - dX(t) \quad (11)$$

Based on isostatic theoretical consideration:

$$C + X(t) = Z = constant \quad (12)$$

and substitution of $C = Z - X(t)$ into Eq. (11) gives Eq. (13) as below:

$$\{[X(t+\delta t) - X(t)]/\delta t\} = c[Z - X(t)]\,X(t) - dX(t) \quad (13)$$

Eq. (13) may be rewritten as an iterative relationships as Eq. (14):

$$X_{n+1} = (aZ - d + 1)X_n - aX_n^2 = \mu X_n - bX_n^2 \quad (14)$$

Where, $\mu = cZ - d + 1$, substituting $X_n = dX_n/\mu$ for Eq. (6), the final Eq. (15) is obtained as below:

$$X_{n+1} = \mu X_n(1 - X_n) \quad (15)$$

Where,

X_n = the potential of structural forces affecting the lithological rock units in step n;

μ = average net reproductive rate of the charges.

Eq. (15) is the real logistic map with simple representation of the quantitative dynamics, shown in Figure (3) as the bifurcation diagram [5]. The solution of this equation is actually sensitive to μ variation. It means that at the intervals $0 < X_n < 1$, the possible assumptions of variances in X_n, are as follows:

- $\mu \le 1$: the value of X_n decrease to 0 as $n \to \infty$.
- $1 < \mu \le 2$, the value of X_n increase to $1-1/\mu$ as $n \to \infty$.
- $2 < \mu \le 3$, the value of X_n fluctuates decreasingly to $1-1/\mu$ as $n \to \infty$.
- $1+\sqrt{6} < \mu \le 4$, the stable value of X_n start to vary complicatedly.

Eq. (15) is valid where the values of X are $0 < X_n < 1$. Since the forces cannot be negative, the above mentioned ranges are $0 < \mu < 4$. There are two types of fixed points at X_0 and $X_0 = 1-1/\mu$. The first points are stable for $0 < \mu < 1$ and unstable for $\mu > 1$; the second ones are stable for $0 < \mu < 3$ and unstable for $\mu > 3$. The main parameters of charging ranges can be described by the logistic maps, see Eq. (15) which cause the discrimination between shallow and deep structures related to seismic epicenters on the basis of similarity formation.

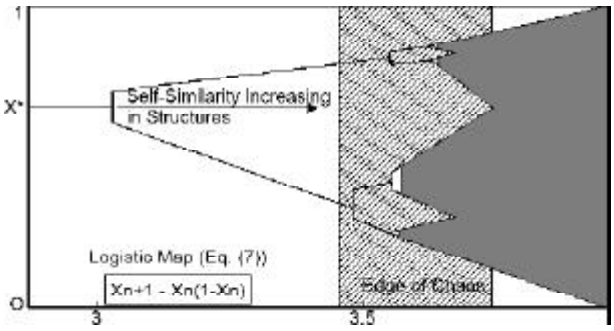

Figure 3. Cantor set diagram showing fractals with bifurcative properties.

The iterative processes comes about chaos for the reproductive values $3.5699 < \mu < 4$. The net values $\mu \le 1$ have no assumptions for hazardous areas as the variables approach zero nearby stable fixed points in a closed system. In the interval $1 < \mu \le 4$, the equation shows active regions with uneven specification of chaotic environments. The values of fixed points are low in the interval $1 < \mu \le 2$ and show low activity of structures. The values of stable points increase in the interval $2 < \mu \le 3$, and the value of stable point is increased indicating the main seismic procedure of extreme stresses (maximum charges) with adequate potential of earthquakes. In the interval $3 < \mu \le 4$, the logistic set begin to multiperiodic cases cause to more non-linearities appearing at the edge of chaos. The alternative charging-discharging processes are important factors in the geological environments due to the rejuvenating of lineaments [6].

The above mentioned phenomenon is not an accidental event subjecting the stochastic random processes. Its profound causes are that the most important historical earthquakes have shown fractal distribution of seismological parameters before and after occurrence. The former can be used for precursory purposes by geologists [2].

Using fractals for simple modeling of complexities indicates the co-evolution of the natural systems

with chaotic behaviors [7]. According to the return periods, processed for some hazardous natural events such as San-Andreas earthquakes [3] and Kilauea volcanic eruptions in Hawaii [8], the results are similar to chaotic maps specified with recursive functions. Therefore, the achievements are applied in the current research for precursory of earthquakes and mentioned in the following.

4. An Overview to Anatolian Earthquakes

In this study, the μ parameter is estimated by Eq. (15) and is applied to a real seismological dataset. This dataset is used in systematic survey of the considered regions, located in the 100*k* sheets Poldasht, eastern Azerbaijan province, *NW* of Iran.

Tabriz, as the center of seismic area, is about $150km^2$. The geological formation of this region is as follows: mainly of late Paleogene limestone (Qom Fm.); Neogene volcanoclastics and Quaternary alluvials as exposed clastic sediments; young intermediate sub-volcanites (Pliocene) ranges rhyodacitic to quartz-diorite domes; felsic igneous units including granodioritic intrusives [9].

The geological structures have mostly been affected by extensional-compressional alternate stresses as the results of taphrogenic movements in association with active fault systems located in the north of Tabriz [10].

According to Figure (4), the main structural branches around the north fault of Tabriz could be originated from Anatolian end members before being extended to the North West territories of Iran [9].

The north Tabriz fault seems to be an active young system with some Quaternary rejuvenation; therefore, it should be considered as the historical catastrophic fault [10].

The region is gridded in eighteen model cells for detecting μ parameter values. According to the results obtained in this research, the seismic values do not increase significantly in the cells with $\mu \leq 2$. However, there are 3 numbers which slowly charge the increased seismic values in the cells with $2 < \mu \leq 3$. This fact indicates the historical events around the north Tabriz fault [9]. Furthermore, two seismic values increase effectively in the cells with $3 < \mu \leq 3.56$; and finally, four essential seismic values increase nearby Anatolian trend. This is the real evidence controlling uneven chaotic behaviors of active regions in the north of Tabriz [11], shown by the cells with $3.56 < \mu \leq 4$.

Here, three geophysical variables, airborne magnetic anomalies [12], gravity dataset [13] and digital number values (originated from satellite images) [14] are used. They are obtained as independent values, Figure (5), in association with seismic

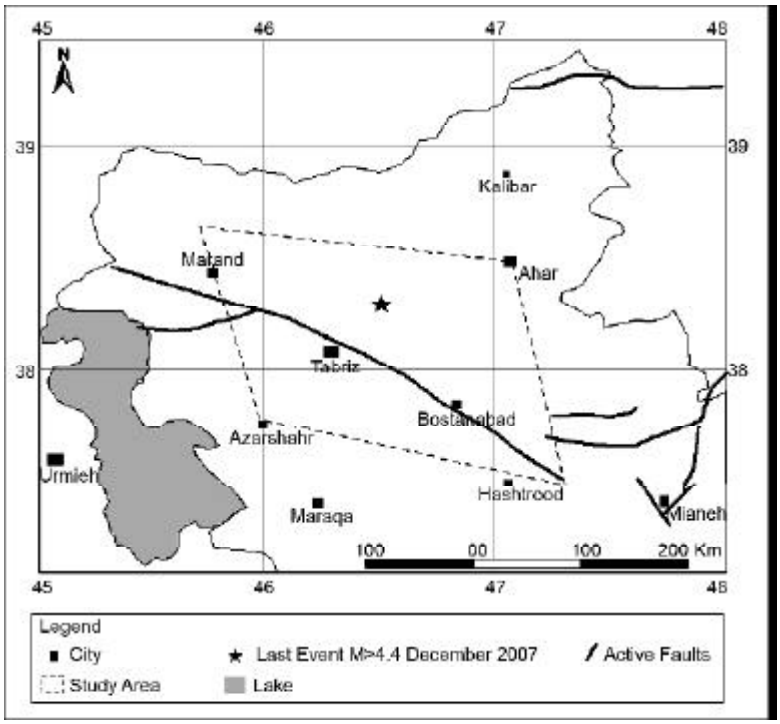

Figure 4. Anatolian fault system related to seismic events in Eastern Azerbaijan province, NW of Iran.

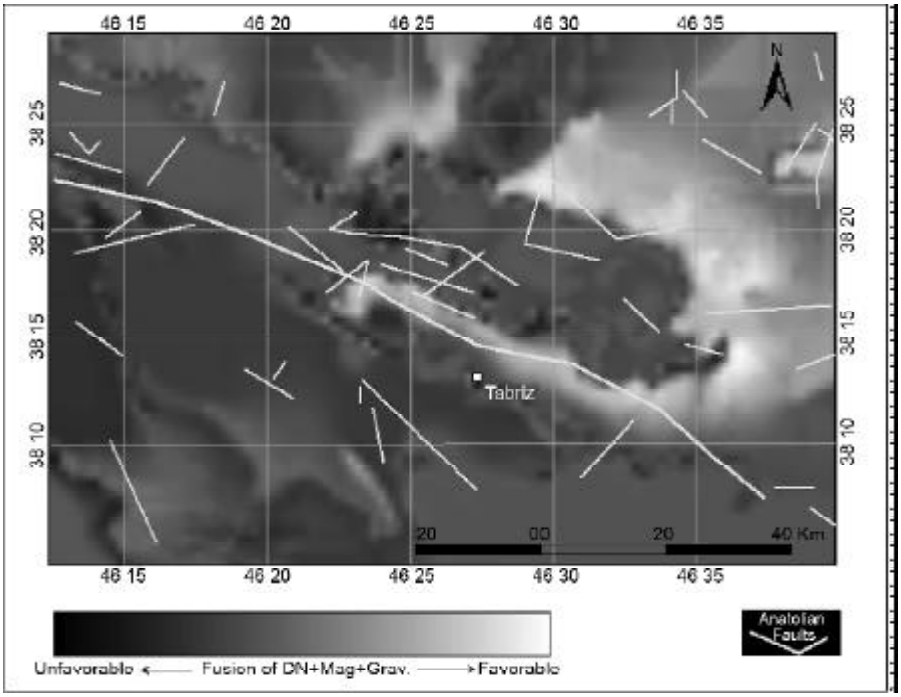

Figure 5. Geophysical evidences related to Anatolian active fault systems, NW of Iran.

alternations within eighteen modeled cells. These cells are gained after net reproducing processes for measuring dependent seismic variables. The variables are presented as real approximated values in Table (1).

The stepwise polynomial regression is obtained by three important geophysical variables and eighteen values of parameter μ in model cells as below:

$$\mu = 1.71 + 1.45_{X1} + 1.63_{X2} + 0.49_{X3} - 0.56_{X1\text{-}2} - 0.16_{X1\text{-}3} + 0.88_{X2\text{-}3} + 0.33_{X1\text{-}2\text{-}3}$$

where,

X_1 = airborne magnetic evidence;
X_2 = airborne gravimetric evidence;
X_3 = remotely sensed evidence;
$X_{1\text{-}2}$ = magnetic and gravimetric evidences;
$X_{1\text{-}3}$ = magnetic and electromagnetic evidences;
$X_{2\text{-}3}$ = gravimetric and electromagnetic evidences;
$X_{1\text{-}2\text{-}3}$ = all geophysical evidences related to historical events.

Based on the above regression equation, the estimators of μ parameter within ten forecasting cells are given in Table (2).

The varieties of these estimators are described as follows:

According to Figure (6), the cell numbers 2, 4, 7, 12, 21 with estimator values >3, may contain the structures with enough potential activities for future earthquakes. These event occur nearby Anatolian systems, followed by recent Tabriz fault branches in three main strikes: N97*E*, N128*E*, N115*E*.

Other cells with forecast values ≤ 3 indicate that approximately stable regions are located far from Anatolian lineaments. Such regions have constraint

Table 1. Value of parameter μ in eighteen model cells.

Cell Number	Value of Parameter μ	Cell Number	Value of Parameter μ
1	2.50	3	3.25
6	3.25	8	3.00
11	2.00	13	2.00
14	2.00	15	3.00
18	3.50	20	3.25
22	2.50	23	3.00
24	3.25	27	2.25
34	2.50	37	3.00
38	3.50	40	3.25

Table 2. Estimators of parameter μ in ten forecast cells.

Cell Number	Forecast Value	Cell Number	Forecast Value
2	3.25	12	3.60
4	3.50	21	3.90
5	3.00	25	2.75
7	3.56	29	2.00
9	2.25	33	3.00

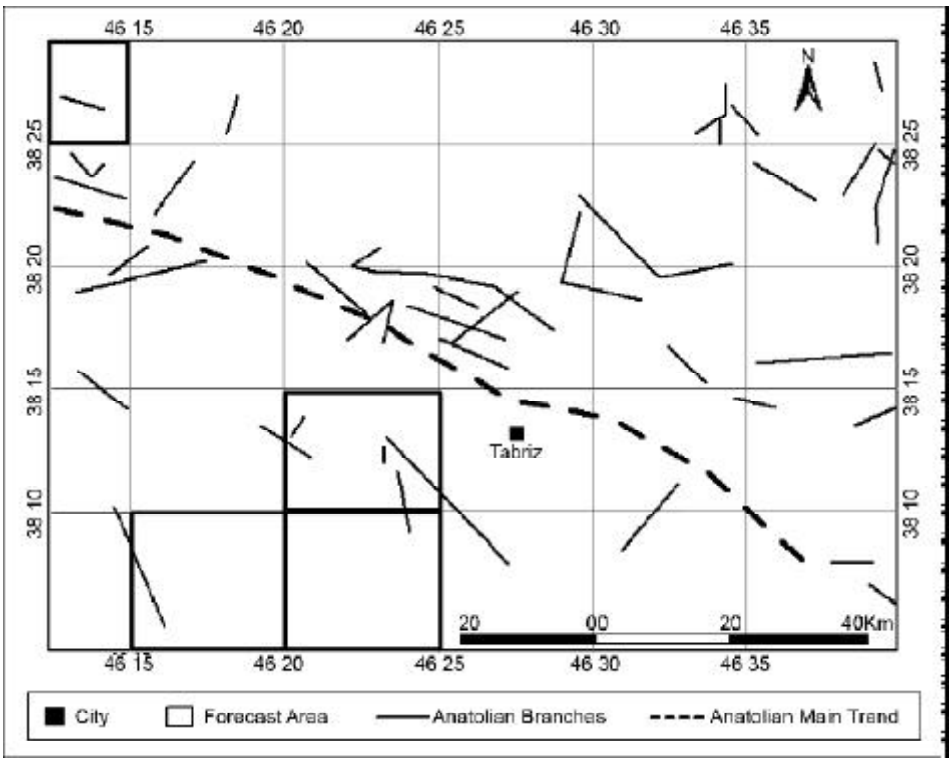

Figure 6. Prognostic map for earthquake prediction based on net reproductive values (μ), NW of Iran.

potentials for occurring limited activities. This fact is due to the deep focal mechanism under geological trapped regions which prohibit the magnitudes from overcharging.

5. Conclusions

Slow charging the interior forces causes sudden movement of fault systems, known as seismic activities in diversity of time, magnitude and locations. Many geophysical measurements are in close relationships with solid state reactions that possess uneven peculiarities through earthquakes. Chaotic dynamic model is a new approach to precursor seismic events based on nonlinearity reigning of parameters and quantities. Logistic maps with recursive functions have been recognized as the basic mathematical model for describing the behavior of earthquakes using fractal properties at the edge of chaos.

As a result, the research regions in the *NW* of Iran have been divided into two zones, active and stable, according to μ parameter values as net reproductive rate of seismic quantities. Estimating μ values during application of real data give rise to successful forecasting cells for $3.56 < \mu \leq 4$. Furthermore, they may suggest the Anatolian trend as the main hazardous structure. This structure may cause nonlinear manifests in the geophysical dataset along the earthquake lineaments with intense background of activities (Table (2), cell numbers 2, 4, and 7) in the north of Tabriz.

Acknowledgements

Here, Payame Noor University is greatly acknowledged for supporting this research by its foundation (Grant no. 2700-88). The author would like to thank Dr. M. Zare for his effective cooperation and Ms. J. Jahromi for editing this paper.

References

1. Mandelbrot, B.B. (1983). "The Fractal Geometry of Nature", Freeman, W.H., New York, 468p.

2. Turcotte, D.L. (1986a). "A Fractal Approach to Relationship between Ore Grade and Tonnage", *Economic Geology*, **81**(6), 1528-1532

3. Turcotte, D.L. (1986b). "Fractal and Fragmentations", *Journal of Geoph. Res.* , **91**, 1921-1926.

4. Yu, Ch. (1999). "Large Ore Deposits and Metallogenic Districts at the Edge of Chaos", *Earth Science Frontiers*, **6**(1-2), 85-102 and 195-230.

5. Turcotte, D.L. (1989). "Fractals in Geology and Geophysics, PAGEOPH", **131**(1/2), 171-196.

6. Agterberg, F.P., Cheng, Q., Brown, A., and Good, D. (1996). "Multifractal Modeling of Fractures in the Lac Du Bonnet Batholith, Manitoba", *Computers and Geosciences*, **22**, 497-507.

7. Tuhua, M., Xingshen, Z., and Changjian, L. (1998). "Chaos Dynamic behaviors of Mineralization", Acta Geologica Sinica, **72**(4), 392-398.

8. Sornette, A., Dubois, J., Cheminee, J.L., and Sornette, D. (1991). "Are Sequences of Volcanic Eruptions Deterministically Chaotic?", *Journal Geophysics Res.*, **96**(11), 931-945.

9. Lescuyer, J. (1978). "Petrology and Petrography of Cenozoic Volcanism in Mianeh Area (East Azerbaijan)", Ph.D. Thesis, University of Paris, Paris, Submitted to Geological Survey of Iran (GSI).

10. Mehrnia, R. (2006). "Using Fractal Strategies for Aeromagnetic Data Positioning Purpose Around North-West Anomalies of Iran", *Proceedings of Map Asia International Conference, GIS Developments*, Thailand, 48-57.

11. Mehrnia, R. (2009). "Using Fractal Filtering Technique for Processing ETM Data as Main Criteria for Evaluating of Gold Indices in NW of Iran", *Proceedings of International Conference on Graphic and Image Processing, ICGIP*, Malaysia, **2**, 298-302.

12. Austirex, Australian Surveying Group (1978). "Aeromagnetic Anomalies in 1/250000 Sketch Map of East Azerbaijan Province, NW of Iran", SN: NJ3812.

13. Enel, Italian Surveying Group (1976). "Boguer Anomalies in 1/250000 Sketch Map of East Azerbaijan Province, NW of Iran", SN: NJ3812.

14. Geological Survey of Iran, Remote Sensing Group (2003). "ETM Images of East Azerbaijan Province, NW of Iran", SN: NJ3812.